

# Chapter 15

## Controlling Parametric Resonance: Induction and Stabilization of Unstable Motions

Roberto Galeazzi and Kristin Y. Pettersen

### 15.1 Parametric Resonance: Threat or Advantage?

Parametric resonance is a well-known resonant phenomenon, which can determine the instability of a system in response to small periodic variations of one of its parameters. In the light of this simple description, the common sense suggests that parametric resonance is a threat for any system where it can potentially onset. As a matter of fact, if we restrain the analysis to marine structures and automotive systems the former answer perfectly fits. For the last 12 years parametric roll resonance on ships has been in focus of the maritime community as one of the top stability related issues, and still it is. Several control strategies have been proposed, which try to stabilize the large roll motion: backstepping controllers have been designed to damp the resonant oscillations using, for example, active U-tanks [5] or fin stabilizers [3]; an extremum seeking controller has been proposed to detune the frequency synchronization by altering ship's speed and/or course [2]. A considerable effort has also been produced by the automotive research community, in particular focusing on how periodic variations of the road profile can induce unstable steering oscillations in motorcycles [8, 13].

However, if we look at a completely different class of systems it is possible to find several applications where the onset of parametric resonance is an advantage.

---

R. Galeazzi (✉)

Department of Electrical Engineering, Technical University of Denmark, DTU Electrical Engineering, DK 2800 Kgs. Lyngby, Denmark

Center for Ships and Ocean Structures, Norwegian University of Science and Technology, NO-7491 Trondheim, Norway

e-mail: [rg@elektro.dtu.dk](mailto:rg@elektro.dtu.dk)

K.Y. Pettersen

Department of Engineering Cybernetics, Norwegian University of Science and Technology, NO-7491 Trondheim, Norway

e-mail: [Kristin.Ytterstad.Pettersen@itk.ntnu.no](mailto:Kristin.Ytterstad.Pettersen@itk.ntnu.no)

In micro-electromechanical systems parametric resonance phenomena are induced in order to, for example, reduce the parasitic signal in capacitive sensing [16], or to increase the sensitivity of mass sensors at the pico scale ( $10^{-12}$  g) [17], or to increase robustness against parameter variations in micro-gyroscopes [12]. Analogous interests in capitalizing the large energy released by parametric resonant oscillations to boost specific system features is also raising in the field of wave energy exploitation. Here the idea is to induce parametric resonance in order to increase the amount of energy producible by the converter [10, 11].

Therefore, by looking at the large variety of systems and possible applications where parametric resonance may naturally occur or can be artificially induced, it appears natural to investigate how active control strategies can be used in order to either trigger the resonant phenomenon or to stabilize it. Starting from this consideration, in this chapter the authors revisit some of the theory of parametric resonance through the use of a mechanical equivalent, which can represent many of the systems aforementioned, and they cast both the induction and the stabilization of resonant oscillations as a tracking problem. An input–output feedback linearizing controller is then designed and shown to be capable both of triggering parametric resonance and stabilizing the unstable motion.

In particular, Sect. 15.2 introduces the mechanical system used in the analysis, namely the pendulum with moving support, as a member of the class of autoparametric systems. Lagrangian description of the system's dynamics is provided, and the stability analysis of the open loop system is carried out. Section 15.3 formulates the control problems, and it presents the design of the controller based on feedback linearization theory. Section 15.4 illustrates the performance of the closed loop system through simulation results. Section 15.5 draws some conclusions, and it highlights possible future research paths.

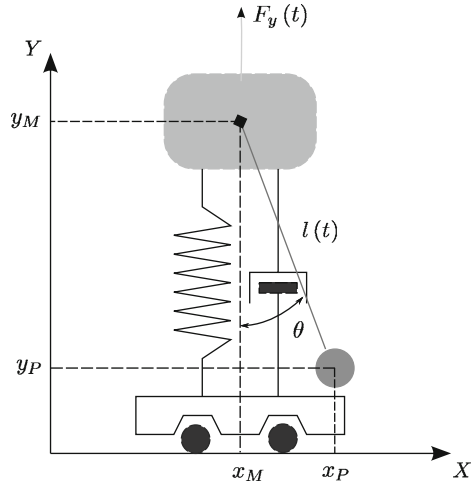
## 15.2 Autoparametric Systems

Autoparametric systems consist of two or more vibrating components, which interact in a nonlinear fashion [14]. The components are divided into the *primary system*, which is usually in a vibrating state, and the *secondary system*, which is usually at rest while the primary system is oscillating. This state is called semi-trivial solution of the autoparametric system.

The excitation acts on the primary system under the form of external forcing, self-excitation, parametric excitation, or a combination of those. Within certain intervals of the excitation frequency the semi-trivial solution can become unstable, and the system enters in autoparametric resonance. The vibrations of the primary system act as parametric excitation on the secondary one, which will be no longer at rest.

Autoparametric systems in resonance condition can display different behaviors including periodic, quasi-periodic, non-periodic, and also chaotic behaviors. Moreover, the occurrence of the resonance often goes along with saturation phenomena. In particular, when the secondary system enters into parametric resonance it

**Fig. 15.1** Pendulum with moving support. The reference frame is right-handed, therefore positive rotations are counterclockwise



functions as an energy absorber by draining energy from the external excitation through the primary system. This entails a large increase of the amplitude of the displacements of the secondary system whereas the oscillation's amplitude of the primary system is maintained as almost constant.

The energy absorbercy of the secondary system can determine both undesirable and desirable results. When parametric roll onsets on a ship, the roll motion becomes the sink of the wave energy exciting the vessel, and the springing of violent roll oscillations is definitely a troublesome outcome. Conversely if the resonance could be induced in a wave energy converter, the capability of draining more energy out of the wave motion will clearly be beneficial.

The difference between autoparametric resonance and parametric resonance resides in the presence of a primary system driving the onset of the resonant condition. For instance parametric roll on ships can be seen as either a parametric resonance or an autoparametric resonance phenomenon depending on whether we consider only the roll subsystem or we include the heave and/or pitch dynamics. In the former case the parametric resonance originates as a result of the quasi-periodic variations of the ship's metacentric height, which is a parameter within the roll dynamics; in the latter case are the oscillations in heave and/or pitch (primary system), directly excited by the wave motion, which determine the onset of the resonant behavior in roll.

### 15.2.1 Pendulum with Moving Support

A well-known autoparametric system is the pendulum with moving support, as that represented in Fig. 15.1. The system consists of a pendulum, whose pivot point is connected to a mass-spring-damper, which in turn is placed atop a cart. The position of the pivot point can change both along the X and Y directions due to

the vertical oscillation of the mass-spring-damper or to the horizontal displacement of the cart. The mass-spring-damper together with the cart represent the primary system, whereas the pendulum is the secondary system. The system is assumed to be underactuated since no direct control action can be performed either on the vertical motion of the mass-spring-damper or on the swinging motion of the pendulum.

The mass-spring-damper is in a vibration state due to the action of an external sinusoidal force; conversely the pendulum's bob is not directly subject to any force/moment apart from gravity, hence the secondary system is initially at rest. In order to induce parametric resonance into the secondary system two conditions must be fulfilled:

- The equilibrium position of the pendulum's bob must be altered.
- The natural frequency of the pendulum must be approximately equal to half the frequency of the external excitation.

Since the swinging of the pendulum cannot be directly actuated due to the absence of a torque acting on the pivot point, the first requirement can be met by changing the position of the cart, which will produce an inertia effect about the pivot point. Considering that the natural frequency of a pendulum is a function of the length of the pendulum's rod, it is evident that in order to achieve the second requirement the pendulum must have a variable length rod.

A four degrees-of-freedom model is first derived by applying Lagrange's theory. Then a stability analysis under the assumption of external sinusoidal excitation is carried out to determine the stability conditions to be infringed in order to trigger the resonant phenomenon.

### 15.2.1.1 Lagrangian Model

Consider a mass-spring-damper system of mass  $m_1$  oscillating under the action of an external sinusoidal force  $F_y(t)$ . A second mass  $m_2$  is attached to the bottom end of a massless rod of variable length, whose pivot point is joint to the first mass  $m_1$ . The two masses are placed on top of a massless cart that is free to move along the horizontal direction.

Said  $l_0$  the nominal length of the pendulum, the variable rod's length is given by

$$l(t) = l_0 + \delta_l(t), \quad \forall t \quad \delta_l(t) > -l_0,$$

where  $\delta_l$  is the deviation from the nominal value. Then the vector of generalized coordinates is defined as  $\mathbf{q} \triangleq [x_M, y_M, \theta, \delta_l]^T$ , where  $(x_M, y_M)$  is the position of the mass  $m_1$ , and  $\theta$  is the oscillation angle of the pendulum.

The equations of motion can be derived from *Lagrange's equations*

$$\frac{d}{dt} \left( \frac{\partial \mathcal{L}(\mathbf{q}, \dot{\mathbf{q}})}{\partial \dot{\mathbf{q}}} \right) - \frac{\partial \mathcal{L}(\mathbf{q}, \dot{\mathbf{q}})}{\partial \mathbf{q}} = \boldsymbol{\tau}, \quad (15.1)$$

where

$$\mathcal{L}(\mathbf{q}, \dot{\mathbf{q}}) = \mathcal{T}(\mathbf{q}, \dot{\mathbf{q}}) - \mathcal{V}(\mathbf{q}) \quad (15.2)$$

is the Lagrangian given by the difference between the kinetic energy  $\mathcal{T}$  and the potential energy  $\mathcal{V}$ ;  $\tau$  is the vector of the generalized forces that accounts for unknown external forces (disturbances)  $\tau^e$  and for control inputs  $\tau^c$

$$\begin{aligned} \tau &= \tau^e + \tau^c \\ &= \begin{bmatrix} 0 \\ F_y^e \\ 0 \\ 0 \end{bmatrix} + \begin{bmatrix} F_x^c \\ 0 \\ 0 \\ F_\delta^c \end{bmatrix}. \end{aligned}$$

Given the position  $(x_M, y_M)$  of the mass  $m_1$ , the position of the mass  $m_2$  at any given instant in time is given by the vector (in the following the notation  $s_\theta$  and  $c_\theta$  stands for  $\sin \theta$  and  $\cos \theta$ , respectively)

$$\mathbf{r}_P : \begin{cases} x_P = x_M + (l_0 + \delta_l) s_\theta \\ y_P = y_M - (l_0 + \delta_l) c_\theta \end{cases}, \quad (15.3)$$

and its velocity by the vector

$$\mathbf{v}_P : \begin{cases} \dot{x}_P = \dot{x}_M + (l_0 + \delta_l) \dot{\theta} c_\theta + \dot{\delta}_l s_\theta \\ \dot{y}_P = \dot{y}_M + (l_0 + \delta_l) \dot{\theta} s_\theta - \dot{\delta}_l c_\theta \end{cases}. \quad (15.4)$$

The kinetic energy of the  $(m_1, m_2)$ -system is then given by

$$\begin{aligned} \mathcal{T}(\mathbf{q}, \dot{\mathbf{q}}) &= \frac{1}{2} \dot{\mathbf{q}}^T \mathbf{M}(\mathbf{q}) \dot{\mathbf{q}} \\ &= \frac{1}{2} m_1 (\dot{x}_M^2 + \dot{y}_M^2) + \frac{1}{2} m_2 (\dot{x}_P^2 + \dot{y}_P^2) \\ &= \frac{1}{2} (m_1 + m_2) (\dot{x}_M^2 + \dot{y}_M^2) + \frac{1}{2} m_2 \left[ (l_0 + \delta_l)^2 \dot{\theta}^2 + \dot{\delta}_l^2 \right. \\ &\quad \left. + 2(l_0 + \delta_l) (\dot{x}_M c_\theta + \dot{y}_M s_\theta) \dot{\theta} + 2\dot{\delta}_l (\dot{x}_M s_\theta - \dot{y}_M c_\theta) \right], \end{aligned} \quad (15.5)$$

where  $\mathbf{M}(\mathbf{q})$  is the mass-inertia matrix

$$\mathbf{M}(\mathbf{q}) = \begin{bmatrix} m_1 + m_2 & 0 & m_2 (l_0 + \delta_l) c_\theta & m_2 s_\theta \\ 0 & m_1 + m_2 & m_2 (l_0 + \delta_l) s_\theta & -m_2 c_\theta \\ m_2 (l_0 + \delta_l) c_\theta & m_2 (l_0 + \delta_l) s_\theta & m_2 (l_0 + \delta_l)^2 & 0 \\ m_2 s_\theta & -m_2 c_\theta & 0 & m_2 \end{bmatrix}$$

$$\mathbf{M}(\mathbf{q}) = \mathbf{M}^T(\mathbf{q});$$

whereas the potential energy reads

$$\mathcal{V}(\mathbf{q}) = \frac{1}{2}ky_M^2 + m_2g(l_0 + \delta_l)(1 - c_\theta) \quad (15.6)$$

with  $k$  being the spring constant of the mass-spring-damper. The Lagrangian is hence given by

$$\begin{aligned} \mathcal{L}(\mathbf{q}, \dot{\mathbf{q}}) &= \frac{1}{2}(m_1 + m_2)(\dot{x}_M^2 + \dot{y}_M^2) + \frac{1}{2}m_2 \left[ (l_0 + \delta_l)^2 \dot{\theta}^2 + \dot{\delta}_l^2 \right. \\ &\quad \left. + 2(l_0 + \delta_l)(\dot{x}_M c_\theta + \dot{y}_M s_\theta) \dot{\theta} + 2\dot{\delta}_l(\dot{x}_M s_\theta - \dot{y}_M c_\theta) \right] - \frac{1}{2}ky_M^2 \\ &\quad - m_2g(l_0 + \delta_l)(1 - c_\theta), \end{aligned} \quad (15.7)$$

which gives rise to the following equations of motion

$$\begin{aligned} (m_1 + m_2)\ddot{x}_M + d_1\dot{x}_M \\ + m_2 \left[ (l_0 + \delta_l)\ddot{\theta}c_\theta - (l_0 + \delta_l)\dot{\theta}^2s_\theta + 2\dot{\delta}_l\dot{\theta}c_\theta + \ddot{\delta}_l s_\theta \right] &= F_x^c, \end{aligned} \quad (15.8)$$

$$\begin{aligned} (m_1 + m_2)\ddot{y}_M + d_2\dot{y}_M + ky \\ + m_2 \left[ (l_0 + \delta_l)\ddot{\theta}s_\theta + (l_0 + \delta_l)\dot{\theta}^2c_\theta + 2\dot{\delta}_l\dot{\theta}s_\theta - \ddot{\delta}_l c_\theta \right] &= F_y^e, \end{aligned} \quad (15.9)$$

$$\begin{aligned} m_2(l_0 + \delta_l)^2\ddot{\theta} + d_3\dot{\theta} + m_2(l_0 + \delta_l)gs_\theta \\ + m_2(l_0 + \delta_l) \left[ \ddot{x}_M c_\theta + \ddot{y}_M s_\theta + 2\dot{\delta}_l\dot{\theta} \right] &= 0 \end{aligned} \quad (15.10)$$

$$\begin{aligned} m_2\ddot{\delta}_l + d_4\dot{\delta}_l \\ - m_2 \left[ (l_0 + \delta_l)\dot{\theta}^2 + \ddot{x}_M s_\theta - \ddot{y}_M c_\theta + g(1 - c_\theta) \right] &= F_\delta^c \end{aligned} \quad (15.11)$$

where linear damping terms  $d_i\dot{q}_i$  have been introduced. System (15.8)–(15.11) can be rewritten in dimensionless form as

$$\ddot{x} + \mu_1\dot{x} + \alpha \left[ (1 + \delta) (\ddot{\theta}c_\theta - \dot{\theta}^2s_\theta) + 2\dot{\delta}\dot{\theta}c_\theta + \ddot{\delta}s_\theta \right] = \Phi_x^c, \quad (15.12)$$

$$\ddot{y} + \mu_2\dot{y} + \omega_y^2y + \alpha \left[ (1 + \delta) (\ddot{\theta}s_\theta + \dot{\theta}^2c_\theta) + 2\dot{\delta}\dot{\theta}s_\theta - \ddot{\delta}c_\theta \right] = \Phi_y^e, \quad (15.13)$$

$$\ddot{\theta} + \frac{\mu_3}{(1 + \delta)^2}\dot{\theta} + \frac{2}{1 + \delta}\dot{\delta}\dot{\theta} + \frac{1}{1 + \delta}(\omega_\theta^2 + \dot{y})s_\theta + \frac{1}{1 + \delta}\dot{x}c_\theta = 0, \quad (15.14)$$

$$\ddot{\delta} + \mu_4\dot{\delta} - (1 + \delta)\dot{\theta}^2 - \dot{y}c_\theta + \dot{x}s_\theta + \omega_\theta^2(1 - c_\theta) = \Phi_\delta^c, \quad (15.15)$$

where

$$x = \frac{x_M}{l_0}, \quad y = \frac{y_M}{l_0}, \quad \delta = \frac{\delta_l}{l_0}$$

and the parameters are given by

$$\begin{aligned} \alpha &= \frac{m_2}{m_1 + m_2}, & \omega_\theta^2 &= \frac{g}{l_0}, & \omega_y^2 &= \frac{k}{m_1 + m_2}, \\ \mu_1 &= \frac{d_1}{m_1 + m_2}, & \mu_2 &= \frac{d_2}{m_1 + m_2}, & \mu_3 &= \frac{d_3}{m_2 l_0^2}, & \mu_4 &= \frac{d_4}{m_2 l_0}, \\ \Phi_x^c &= \frac{F_x^c}{(m_1 + m_2) l_0}, & \Phi_y^e &= \frac{F_y^e}{(m_1 + m_2) l_0}, & \Phi_\delta^c &= \frac{F_\delta^c}{m_2 l_0}. \end{aligned}$$

By means of matrix notation the following compact form can be achieved (the symbol  $\tilde{\cdot}$  denotes non-dimensional quantities)

$$\tilde{\mathbf{M}}(\tilde{\mathbf{q}}) \ddot{\tilde{\mathbf{q}}} + \tilde{\mathbf{D}} \dot{\tilde{\mathbf{q}}} + \tilde{\mathbf{C}}(\tilde{\mathbf{q}}, \dot{\tilde{\mathbf{q}}}) \dot{\tilde{\mathbf{q}}} + \tilde{\mathbf{g}}(\tilde{\mathbf{q}}) = \tilde{\boldsymbol{\tau}}, \quad (15.16)$$

where  $\tilde{\mathbf{q}} = [x, y, \theta, \delta]^T$ , and  $\tilde{\boldsymbol{\tau}} = [\Phi_x^c, \Phi_y^e, 0, \Phi_\delta^c]^T$ .  $\tilde{\mathbf{M}}(\tilde{\mathbf{q}})$  is the scaled mass-inertia matrix

$$\tilde{\mathbf{M}}(\tilde{\mathbf{q}}) = \begin{bmatrix} 1 & 0 & \alpha(1+\delta)c_\theta & \alpha s_\theta \\ 0 & 1 & \alpha(1+\delta)s_\theta & -\alpha c_\theta \\ (1+\delta)c_\theta & (1+\delta)s_\theta & (1+\delta)^2 & 0 \\ s_\theta & -c_\theta & 0 & 1 \end{bmatrix},$$

$\tilde{\mathbf{D}}$  is the viscous damping matrix

$$\tilde{\mathbf{D}} = \begin{bmatrix} \mu_1 & 0 & 0 & 0 \\ 0 & \mu_2 & 0 & 0 \\ 0 & 0 & \mu_3 & 0 \\ 0 & 0 & 0 & \mu_4 \end{bmatrix}, \quad \tilde{\mathbf{D}} > 0,$$

$\tilde{\mathbf{C}}(\tilde{\mathbf{q}}, \dot{\tilde{\mathbf{q}}})$  is the Coriolis-centripetal matrix

$$\tilde{\mathbf{C}}(\tilde{\mathbf{q}}, \dot{\tilde{\mathbf{q}}}) = \begin{bmatrix} 0 & 0 & -\alpha \left( (1+\delta) \dot{\theta} s_\theta - \dot{\delta} c_\theta \right) & \alpha \dot{\theta} c_\theta \\ 0 & 0 & \alpha \left( (1+\delta) \dot{\theta} c_\theta + \dot{\delta} s_\theta \right) & \alpha \dot{\theta} s_\theta \\ 0 & 0 & (1+\delta) \dot{\delta} & (1+\delta) \dot{\theta} \\ 0 & 0 & -(1+\delta) \dot{\theta} & 0 \end{bmatrix},$$

and  $\tilde{\mathbf{g}}(\tilde{\mathbf{q}})$  is the vector of gravitational-restoring forces and moments

$$\tilde{\mathbf{g}}(\tilde{\mathbf{q}}) = \begin{bmatrix} 0 \\ \omega_y^2 y \\ (1 + \delta) \omega_\theta^2 s_\theta \\ \omega_\theta^2 (1 - c_\theta) \end{bmatrix}.$$

### 15.2.2 Stability Analysis

In this section, a stability analysis under the assumption of external sinusoidal excitation is carried out, to determine the conditions to be infringed in order to trigger the resonant phenomenon.

Consider the mass-spring-damper (15.13) driven by  $\Phi_y^c = \Phi_0 \cos \omega_e t$ , and no control action is performed, that is  $\Phi_x^c = \Phi_\delta^c = 0$ . Then the semi-trivial solution of the system (15.12)–(15.15) is given by

$$x(t) = 0, \quad (15.17)$$

$$y(t) = Y_0 \cos(\omega_e t + \psi_y), \quad (15.18)$$

$$\theta(t) = 0, \quad (15.19)$$

$$\delta(t) = \Delta_0 \cos(\omega_e t + \psi_\delta), \quad (15.20)$$

where the pairs of parameters  $(Y_0, \psi_y)$  and  $(\Delta_0, \psi_\delta)$  can be found by substituting (15.18) and (15.20) into the linear system

$$\ddot{y} + \mu_2 \dot{y} + \omega_y^2 y - \alpha \ddot{\delta} = \Phi_0 \cos \omega_e t, \quad (15.21)$$

$$\ddot{\delta} + \mu_4 \dot{\delta} - \dot{y} = 0. \quad (15.22)$$

The stability of the semi-trivial solution is investigated by looking at its behavior in a neighborhood defined as

$$x(t) = 0 + u_x(t), \quad (15.23)$$

$$y(t) = Y_0 \cos \omega_e t + u_y(t), \quad (15.24)$$

$$\theta(t) = 0 + u_\theta(t), \quad (15.25)$$

$$\delta(t) = \Delta_0 \cos \omega_e t + u_\delta(t), \quad (15.26)$$

where  $u_x(t)$ ,  $u_y(t)$ ,  $u_\theta(t)$ , and  $u_\delta(t)$  are small perturbations, and the phase shifts  $\psi_y$  and  $\psi_\delta$  have been arbitrarily set to zero. Substituting (15.23)–(15.26) into the system (15.12)–(15.15) and linearizing around the semi-trivial solution the following variational system in nondimensional time  $\zeta = \frac{1}{2} \omega_e t$  is obtained



$$u_x'' + \tilde{\mu}_1 u_x' - \alpha (\sigma - 2\tilde{\mu}_4 \Delta_0 \sin(2\zeta)) u_\theta - \frac{\alpha \tilde{\mu}_3}{1 + \Delta_0 \cos(2\zeta)} u_\theta' = 0, \quad (15.27)$$

$$u_y'' + \tilde{\mu}_2 u_y' + \frac{4\omega_y^2}{\omega_e^2} u_y + \tilde{\mu}_4 u_\delta' = 0, \quad (15.28)$$

$$u_\theta'' + \frac{1}{1 + \Delta_0 \cos(2\zeta)} \left[ \left( \frac{\tilde{\mu}_3}{1 + \Delta_0 \cos(2\zeta)} + 4(1 - \alpha) \Delta_0 \sin(2\zeta) \right) u_\theta' + (\sigma + \varepsilon \cos(2\zeta)) u_\theta - \tilde{\mu}_1 u_x' \right] = 0, \quad (15.29)$$

$$u_\delta'' + \tilde{\mu}_4 u_\delta' + \tilde{\mu}_2 u_y' + \frac{4\omega_y^2}{\omega_e^2} u_y = 0. \quad (15.30)$$

where  $\sigma = \frac{4\omega_\theta^2}{\omega_e^2}$ ,  $\varepsilon = \frac{4Y_0}{\omega_e^2}$ , and  $\tilde{\mu}_i = \frac{2\mu_i}{\omega_e}$ . Equations (15.28) and (15.30) form a marginally stable linear system whose solution  $(u_y, u_\delta)$  converges to  $(0, \bar{u}_\delta)$  for  $\zeta$  going to infinity. Therefore the stability of the overall system is solely determined by the  $(u_x, u_\theta)$ -subsystem.

The  $(u_x, u_\theta)$ -subsystem (15.27) and (15.29) is a linear periodic system of the form

$$\dot{\mathbf{z}} = \mathbf{A}(\zeta) \mathbf{z}, \quad \mathbf{A}(\zeta + T) = \mathbf{A}(\zeta), \quad (15.31)$$

where  $\mathbf{z} = [u_x, u_x', u_\theta, u_\theta']^T$ , and the time-varying dynamical matrix  $\mathbf{A}(t)$  is

$$\mathbf{A}(\zeta) = \begin{bmatrix} 0 & 1 & 0 & 0 \\ 0 & -\tilde{\mu}_1 & \alpha (\sigma - 2\tilde{\mu}_4 \Delta_0 \sin(2\zeta)) & \frac{\alpha \tilde{\mu}_3}{1 + \Delta_0 \cos(2\zeta)} \\ 0 & 0 & 1 & 0 \\ 0 & \frac{\tilde{\mu}_1}{1 + \Delta_0 \cos(2\zeta)} & -\frac{\sigma + \varepsilon \cos(2\zeta)}{1 + \Delta_0 \cos(2\zeta)} & -\frac{\tilde{\mu}_3}{(1 + \Delta_0 \cos(2\zeta))^2} - \frac{4(1 - \alpha) \Delta_0 \sin(2\zeta)}{1 + \Delta_0 \cos(2\zeta)} \end{bmatrix}, \quad (15.32)$$

whose entries are periodic functions of period  $T = \pi$ . According to Floquet theory [4] the system (15.31) admits three different kinds of solutions, that is stable, unstable, or periodic, depending on the characteristic multipliers associated to the system. Further, the overall stability of the  $(u_x, u_\theta)$ -subsystem relies on the stability of the  $u_\theta$  dynamics as shown by (15.27), which admits a solution  $u_x \neq 0$  only if  $u_\theta \neq 0$ .

If we assume that  $\Delta_0 \ll 1$  then (15.29) reduces to the linear damped Mathieu equation [9] linked to the cart dynamics through a velocity coupling. Therefore, it is plausible that the stability properties of the  $u_\theta$  dynamics are quite similar to those of the Mathieu equation with damping. In order to confirm this assumption the Fourier spectral method [1, 15] is applied to numerically derive the stability chart of the system (15.31).

Figure 15.2 shows the stability diagram around the first region of instability derived for the following values of the system's parameters:  $\tilde{\mu}_1 = 0.5$ ,  $\tilde{\mu}_3 = 0.1$ ,  $\tilde{\mu}_4 = 0.8$ ,  $\Delta_0 = 0.02$ ,  $\alpha \approx 0.09$ . In particular, the dash-dotted lines are the transition

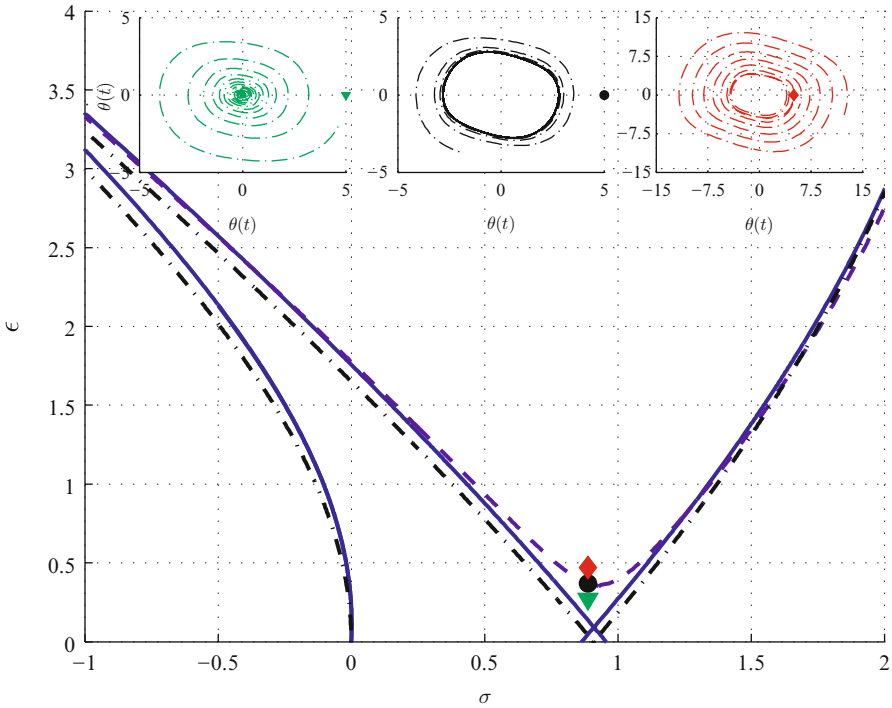


**Fig. 15.2** Stability diagram of the  $(u_x, u_\theta)$ -subsystem: stable, periodic, and unstable solutions can alternate depending upon the value of the parameter set  $(\sigma, \epsilon)$

curves of the linear Mathieu equation coupled with the cart dynamics with  $\tilde{\mu}_i = 0$ ; the solid lines are the transition curves of system (15.31) with  $\tilde{\mu}_i = 0$ ; the dashed lines are the transition curves of system (15.31) with damping coefficients equal to the values above mentioned.

By comparing the transition curves of the linear Mathieu equation (dash-dotted lines) with those of system (15.31) when damping is not included (solid lines) we can see that the effect of the time-varying rod length is to slightly push up the origin of the unstable tongue detaching it from the  $\sigma$ -axis. Moreover, as for the standard damped Mathieu equation, the effect of the damping is to increase the size of the stable regions. As expected, system (15.31) shows three different behaviors: stable if the  $(\sigma, \epsilon)$  pair is below the transition curve; periodic if the  $(\sigma, \epsilon)$  pair lies on the transition curve; unstable if the  $(\sigma, \epsilon)$  pair is above the transition curves. The three different scenarios are illustrated in the inserts within Fig. 15.2.

Concluding, the stability of the  $(u_x, u_\theta)$ -subsystem is determined by three parameters: the frequency tuning  $\sigma$ , which has to be close to 1 (i.e.  $\omega_\theta \approx \frac{1}{2}\omega_e$ ) in the first region of instability; the system damping, which defines the smallest amplitude of the parametric excitation needed in order to trigger the resonance; the amplitude of the parametric excitation  $\epsilon$ , which determines the magnitude of the system response.

## 15.3 Parametric Resonance Control

As the stability analysis pointed out, parametric resonance is an instability phenomenon, whose onset is due to the concurrent fulfillment of two conditions:

- The frequency of the parametric excitation is approximately equal to twice the natural frequency of the secondary system (principal parametric resonance condition).
- The amplitude of the parametric excitation is larger than the damping of the secondary system.

Moreover, the secondary system must be perturbed from its stable equilibrium point in order to trigger the resonance.

Control strategies aiming at stabilizing or inducing parametric resonance into the system have to act on the primary or secondary system such that the aforementioned conditions are failed or met, respectively. It is worth to note that the stabilization of parametric resonance can be achieved by not satisfying only one of the requirements, for example increasing the damping of the secondary system; however by failing both of them a faster convergence to a stable mode is obtained. Conversely, the induction of parametric resonance requires that both prerequisites are attained.

The authors decided to focus on the frequency coupling condition in order to both induce and stabilize the resonant oscillations, assuming that the damping condition is implicitly satisfied. In particular, the induction of parametric resonance is achieved by bringing the system into the principal parametric resonance region, that is, where  $\omega_\theta = \frac{1}{2}\omega_e$ .

### 15.3.1 Parametric Resonance Induction

Assuming that the frequency of the external excitation  $\omega_e$  acting on the mass-spring-damper is retrievable by means of low-level signal processing, the induction of parametric resonance into the system (15.16) can be set up as an *output tracking problem*.

**Problem 15.1.** Let  $\omega_1(t) = \frac{1}{2}\omega_e$  be the induction reference frequency at time  $t$ . Find a control law  $\Phi_\delta^c = \Phi_\delta^c(\tilde{\mathbf{q}}, \dot{\tilde{\mathbf{q}}}, \omega_1(t))$  such that  $\omega_\theta$  converges asymptotically to the prescribed reference frequency trajectory  $\omega_1(t)$ .

The solution of the output tracking problem results in designing the control law  $\Phi_\delta^c$  such that the length of the pendulum rod  $\delta$  converges to  $\delta^*$  for  $t \rightarrow \infty$ , where  $\delta^* = (4l_e - l_0)/l_0$  with  $l_e$  being the length of the rod of a virtual pendulum oscillating at the natural frequency  $\omega_e$ . However this control action alone is not sufficient to trigger parametric resonance; in fact a small perturbation is necessary to bring the pendulum away from its stable equilibrium point  $\theta = 0$ . Problem 15.1 can then be reformulated as

**Parametric Resonance Tracking.** Given the system (15.16) and the induction reference frequency  $\omega_1(t)$ , find a control law  $\tilde{\tau}^c = [\Phi_x^c(\tilde{\mathbf{q}}, \dot{\tilde{\mathbf{q}}}, x^*), \Phi_\delta^c(\tilde{\mathbf{q}}, \dot{\tilde{\mathbf{q}}}, \omega_1(t))]^T$  such that  $\omega_\theta$  converges asymptotically to the prescribed frequency  $\omega_1(t)$ , and  $\theta(t) \neq 0$  for all  $t > t_c$ , where  $t_c$  is the time instant where the control action starts.

The second control goal is achieved by arbitrarily changing the position of the cart along the  $X$  axis, with no specific preference about the value of the new set point or the direction of the motion. Therefore the controller goal in this case is limited to stabilize the cart around the new chosen position  $x^*$ .

Consider the multivariable nonlinear system described in state space form as

$$\dot{\mathbf{x}} = \mathbf{f}(\mathbf{x}) + \mathbf{b}(\mathbf{x})\mathbf{u} + \mathbf{p}(\mathbf{x})\mathbf{w}, \quad (15.33)$$

$$\mathbf{y} = \mathbf{h}(\mathbf{x}) \quad (15.34)$$

in which  $\mathbf{x}$  is the state vector split into the position  $\mathbf{x}_1 = [x_1, x_2, x_3, x_4]^T \triangleq [x, y, \theta, \delta]^T$  and the velocity  $\mathbf{x}_2 = [x_5, x_6, x_7, x_8]^T \triangleq [\dot{x}, \dot{y}, \dot{\theta}, \dot{\delta}]^T$ ,  $\mathbf{u} = [\Phi_x^c, \Phi_\delta^c]^T$  is the vector of control inputs,  $\mathbf{w} = \Phi_y^e$  is the disturbance. The following smooth vector fields defined in an open set of  $\mathbb{R}^8$

$$\begin{aligned} \mathbf{f}(\mathbf{x}) &\triangleq \begin{bmatrix} \mathbf{x}_2 \\ -\tilde{\mathbf{M}}(\mathbf{x}_1)^{-1}(\tilde{\mathbf{D}}\mathbf{x}_2 + \tilde{\mathbf{C}}(\mathbf{x}_1, \mathbf{x}_2)\mathbf{x}_2 + \tilde{\mathbf{g}}(\mathbf{x}_1)) \end{bmatrix}, \\ \mathbf{b}(\mathbf{x}) &\triangleq \frac{1}{1-\alpha} \begin{bmatrix} 0 & 0 & 0 & 0 & 1 & 0 & -\frac{\cos x_3}{1+x_4} & -\sin x_3 \\ 0 & 0 & 0 & 0 & -\alpha \sin x_3 & \alpha \cos x_3 & 0 & 1 \end{bmatrix}^T, \\ \mathbf{p}(\mathbf{x}) &\triangleq \frac{1}{1-\alpha} \begin{bmatrix} 0, 0, 0, 0, 0, 0, 1, -\frac{\sin x_3}{1+x_4}, \cos x_3 \end{bmatrix}^T \end{aligned}$$

describe the state dynamics, whereas the smooth functions

$$\mathbf{h}(\mathbf{x}) \triangleq [x_1, x_4]^T$$

describe the output evolution.

**Proposition 15.1.** *The transformation of variables*

$$\begin{aligned} \mathbf{z} = \begin{bmatrix} \xi \\ \eta \end{bmatrix} &= \mathbf{T}(\mathbf{x}) \\ &= \begin{bmatrix} x_1 \\ x_5 \\ x_4 \\ x_8 \\ x_2 \\ x_3 \\ \frac{\alpha x_8 \cos x_3 - \alpha(1+x_4)x_7 \sin x_3 - x_6}{\alpha \cos x_3} \\ x_7 + \frac{x_5 \cos x_3 + x_6 \sin x_3}{1+x_4} \end{bmatrix} \end{aligned} \quad (15.35)$$

is a local diffeomorphism on the domain  $D_x = \left\{ \mathbf{x} \in \mathbb{R}^8 \mid x_3 \neq \frac{\pi}{2} + n\pi \wedge x_3 \neq \arcsin\left(\alpha^{-\frac{1}{2}}\right) \wedge x_4 \neq -1 \right\}$ , which brings the system (15.33)–(15.34) into the normal form

$$\dot{\eta} = \mathbf{f}_0(\eta, \xi), \quad (15.36)$$

$$\dot{\xi} = \mathbf{A}_c \xi + \mathbf{B}_c \Gamma(\mathbf{x})[\mathbf{u} - \mathbf{v}(\mathbf{x}) - \mathbf{v}(\mathbf{x})], \quad (15.37)$$

$$\mathbf{y} = \mathbf{C}_c \xi, \quad (15.38)$$

where  $\xi \in \mathbb{R}^4$ ,  $\eta \in \mathbb{R}^4$ , and  $(\mathbf{A}_c, \mathbf{B}_c, \mathbf{C}_c)$  is a canonical form representation of a chain of integrators.

*Proof.* The transformation of variables  $\mathbf{T}(\mathbf{x})$  is obtained by exploiting the notion of vector relative degree and applying Proposition 5.1.2 in [6]. System (15.33)–(15.34) has vector relative degree  $\{\rho_1, \rho_2\} = \{2, 2\}$  on the domain  $D_1 = \left\{ \mathbf{x} \in \mathbb{R}^8 \mid x_3 \neq \arcsin\left(\alpha^{-\frac{1}{2}}\right) \right\}$ ; in fact by using the Lie derivative we obtain

$$L_{b_j} h_i = 0, \quad \text{for } 1 \leq j \leq 2, 1 \leq i \leq 2$$

and

$$L_{b_1} L_f h_1(\mathbf{x}) = \frac{1}{1 - \alpha}, \quad (15.39)$$

$$L_{b_1} L_f h_2(\mathbf{x}) = -\frac{\sin x_3}{1 - \alpha}, \quad (15.40)$$

$$L_{b_2} L_f h_1(\mathbf{x}) = -\frac{\alpha \sin x_3}{1 - \alpha}, \quad (15.41)$$

$$L_{b_2} L_f h_2(\mathbf{x}) = \frac{1}{1 - \alpha}. \quad (15.42)$$

Moreover the matrix

$$\begin{aligned} \Gamma(\mathbf{x}) &= \begin{bmatrix} L_{b_1} L_f h_1(\mathbf{x}) & L_{b_2} L_f h_1(\mathbf{x}) \\ L_{b_1} L_f h_2(\mathbf{x}) & L_{b_2} L_f h_2(\mathbf{x}) \end{bmatrix} \\ &= \begin{bmatrix} \frac{1}{1 - \alpha} & -\frac{\alpha \sin x_3}{1 - \alpha} \\ -\frac{\sin x_3}{1 - \alpha} & \frac{1}{1 - \alpha} \end{bmatrix} \end{aligned} \quad (15.43)$$

is nonsingular on  $D_1$ , since its determinant

$$\det(\Gamma(\mathbf{x})) = \frac{1 - \alpha \sin^2 x_3}{(1 - \alpha)^2}$$

is zero if  $x_3 = \arcsin\left(\alpha^{-\frac{1}{2}}\right)$ . Therefore we can define the first four new variables as

$$\xi_1 \triangleq h_1(\mathbf{x}) = x_1, \quad (15.44)$$

$$\xi_2 \triangleq L_f h_1(\mathbf{x}) = x_5, \quad (15.45)$$

$$\xi_3 \triangleq h_2(\mathbf{x}) = x_4, \quad (15.46)$$

$$\xi_4 \triangleq L_f h_2(\mathbf{x}) = x_8. \quad (15.47)$$

Since  $\rho = \rho_1 + \rho_2 = 4$  and the state space is eight dimensional, it is possible to find four other functions  $\eta_i(\mathbf{x})$  such that the mapping

$$\mathbf{T}(\mathbf{x}) = [\xi_1, \dots, \xi_4, \eta_1, \dots, \eta_4]^T$$

is a local diffeomorphism. By noting that the distribution  $B = \text{span}\{b_1, b_2\}$  is involutive on  $D_1$ , we can determine the functions  $\eta_i$  by solving the set of linear partial differential equations

$$\begin{aligned} L_{b_j} \eta_i(\mathbf{x}) &= 0 \\ \Rightarrow \begin{cases} \frac{\partial \eta_i}{\partial x_5} - \frac{\cos x_3}{1+x_4} \frac{\partial \eta_i}{\partial x_7} - \sin x_3 \frac{\partial \eta_i}{\partial x_8} &= 0 \\ -\alpha \sin x_3 \frac{\partial \eta_i}{\partial x_5} + \alpha \cos x_3 \frac{\partial \eta_i}{\partial x_6} + \frac{\partial \eta_i}{\partial x_8} &= 0 \end{cases} \end{aligned} \quad (15.48)$$

A set of functions satisfying system (15.48) is given by

$$\eta_1 \triangleq x_2, \quad (15.49)$$

$$\eta_2 \triangleq x_3, \quad (15.50)$$

$$\eta_3 \triangleq \frac{\alpha x_8 \cos x_3 - \alpha(1+x_4)x_7 \sin x_3 - x_6}{\alpha \cos x_3}, \quad (15.51)$$

$$\eta_4 \triangleq x_7 + \frac{x_5 \cos x_3 + x_6 \sin x_3}{1+x_4}. \quad (15.52)$$

which is defined on the domain  $D_2 = \{\mathbf{x} \in \mathbb{R}^8 \mid x_3 \neq \frac{\pi}{2} + n\pi \wedge x_4 \neq -1\}$ . Therefore, the change of variables (15.35) qualifies as a diffeomorphism since its jacobian matrix is nonsingular on the domain  $D_x = D_1 \cap D_2$ .

Finally by applying the transformation  $\mathbf{T}(\mathbf{x})$  to the system (15.33)–(15.34) we obtain the normal form (15.36)–(15.38) where  $\Gamma(\mathbf{x})$  is given by (15.43) and

$$\begin{aligned}
\mathbf{v}(\mathbf{x}) &= \begin{bmatrix} L_f^2 h_1(\mathbf{x}) \\ L_f^2 h_2(\mathbf{x}) \end{bmatrix} \\
&= \begin{bmatrix} \frac{1}{1-\alpha} \left( -\mu_1 x_5 + \alpha \mu_4 x_8 \sin x_3 + \frac{\alpha \mu_3}{1+x_4} x_7 \cos x_3 + \alpha \omega_\theta^2 \sin x_3 \right) \\ \frac{1}{1-\alpha} \left( -\mu_4 x_8 + \mu_1 x_5 \sin x_3 - \mu_2 x_6 \cos x_3 \right. \\ \left. + (1-\alpha)(1+x_4)x_7^2 - \omega_\theta^2(1-\cos x_3) - \omega_\gamma^2 x_2 \cos x_3 \right) \end{bmatrix}, \tag{15.53}
\end{aligned}$$

$$\begin{aligned}
\mathbf{v}(\mathbf{x}) &= \begin{bmatrix} L_p L_f h_1(\mathbf{x}) \\ L_p L_f h_2(\mathbf{x}) \end{bmatrix} \\
&= \begin{bmatrix} 0 \\ \cos x_3 \\ 1-\alpha \end{bmatrix}. \tag{15.54}
\end{aligned}$$

□

Equation (15.54) shows that the disturbance  $\Phi_y^e$  affects the output  $y_2$ , whereas the output  $y_1$  is insensitive to it. Hence the control design should also address the problem of disturbance decoupling together with the tracking of parametric resonance.

**Proposition 15.2.** *Consider the system in normal form (15.36)–(15.38), and the reference vector  $\mathbf{y}_R = [y_{1R}(t), \dot{y}_{1R}(t), y_{2R}(t), \dot{y}_{2R}(t)]^T = [x_1^*(t), x_5^*(t), x_4^*(t), x_8^*(t)]^T$ . The input–output feedback linearizing control law*

$$\mathbf{u} = \Gamma(\mathbf{x})^{-1}(\mathbf{v}(\mathbf{x}) + \mathbf{v}(\mathbf{x})\mathbf{w} + \phi(\mathbf{x})),$$

where

$$\phi(\mathbf{x}) = \mathbf{v} + \ddot{\mathbf{y}}_R(t)$$

solves the Parametric Resonance Tracking problem and decouples the disturbance from the output  $y_2$ . Moreover, the internal dynamics  $\dot{\eta} = \mathbf{f}_0(\eta, \xi)$  is bounded for all  $t \geq 0$ .

*Proof.* Let

$$\mathbf{e} = \begin{bmatrix} \xi_1 - y_{1R}(t) \\ \xi_2 - \dot{y}_{1R}(t) \\ \xi_3 - y_{2R}(t) \\ \xi_4 - \dot{y}_{2R}(t) \end{bmatrix} = \xi - \mathbf{y}_R$$

be the tracking error vector. Introducing the tracking error into the normal form (15.36) and (15.37) yields

$$\dot{\eta} = \mathbf{f}_0(\eta, \mathbf{e} + \mathbf{y}_R), \tag{15.55}$$

$$\dot{\mathbf{e}} = \mathbf{A}_c \mathbf{e} + \mathbf{B}_c \Gamma(\mathbf{x}) \left\{ [\mathbf{u} - \mathbf{v}(x) - \mathbf{v}(\mathbf{x})] - \begin{bmatrix} \ddot{y}_{1R} \\ \ddot{y}_{2R} \end{bmatrix} \right\}. \tag{15.56}$$

Hence the state feedback control

$$\mathbf{u} = \Gamma(\mathbf{x})^{-1}(v(\mathbf{x}) + v(\mathbf{x})\mathbf{w} + \phi(\mathbf{x})) \quad (15.57)$$

reduces the system (15.36)–(15.37) to the cascade system

$$\dot{\eta} = \mathbf{f}_0(\eta, \mathbf{e} + \mathbf{y}_R), \quad (15.58)$$

$$\dot{\mathbf{e}} = \mathbf{A}_c \mathbf{e} + \mathbf{B}_c \phi(\mathbf{x}), \quad (15.59)$$

where

$$\phi(\mathbf{x}) = -\mathbf{K}_I \mathbf{e} + \begin{bmatrix} \ddot{y}_{1R} \\ \ddot{y}_{2R} \end{bmatrix}. \quad (15.60)$$

By selecting the gain matrix  $\mathbf{K}_I$  such that the matrix  $\mathbf{A}_c - \mathbf{B}_c \mathbf{K}_I$  is Hurwitz, then the *Parametric Resonance Tracking* problem is solved.

The normal form (15.36) and (15.37) has an equilibrium point at  $(\eta, \xi) = (0, 0)$ . In particular, the zero dynamics  $\dot{\eta} = \mathbf{f}_0(\eta, 0)$  given by

$$\dot{\eta}_1(\eta, 0) = -\frac{\alpha \eta_3 \cos \eta_2 + \alpha \eta_4 \sin \eta_2}{1 - \alpha \sin^2 \eta_2}, \quad (15.61)$$

$$\dot{\eta}_2(\eta, 0) = \frac{\eta_4 + \frac{1}{2} \alpha \eta_3 \sin(2\eta_2)}{1 - \alpha \sin^2 \eta_2}, \quad (15.62)$$

$$\begin{aligned} \dot{\eta}_3(\eta, 0) &= \frac{\mu_2(\eta_3 \cos \eta_2 + \eta_4 \sin \eta_2)}{(\alpha \sin^2 \eta_2 - 1) \cos \eta_2} - \frac{(\eta_4 + \frac{1}{2} \alpha \eta_3 \sin(2\eta_2)) \eta_3 \sin(2\eta_2)}{2(\alpha \sin^2 \eta_2 - 1) \cos \eta_2} \\ &\quad + \frac{\omega_y^2 \eta_1}{\alpha \cos \eta_2}, \end{aligned} \quad (15.63)$$

$$\begin{aligned} \dot{\eta}_4(\eta, 0) &= \frac{\eta_4 + \frac{1}{2} \alpha \eta_3 \sin(2\eta_2)}{\alpha \sin^2 \eta_2 - 1} \left( \mu_3 - \frac{(\eta_3 \cos \eta_2 + \eta_4 \sin \eta_2) \alpha \cos \eta_2}{\alpha \sin^2 \eta_2 - 1} \right) \\ &\quad - \omega_\theta^2 \sin \eta_2 \end{aligned} \quad (15.64)$$

is locally asymptotically stable in  $\eta = 0$ . In fact by linearizing the zero dynamics around  $\eta = 0$  we obtain the following matrix

$$\mathbf{A}_0 = \begin{bmatrix} 0 & 0 & -\alpha & 0 \\ 0 & 0 & 0 & 1 \\ \frac{\omega_y^2}{\alpha} & 0 & -\mu_2 & 0 \\ 0 & -\omega_\theta^2 & 0 & -\mu_3 \end{bmatrix}, \quad (15.65)$$



whose eigenvalues

$$\lambda_{1,2} = -\frac{1}{2}\mu_2 \pm \sqrt{\mu_2^2 - 4\omega_y^2}, \quad (15.66)$$

$$\lambda_{3,4} = -\frac{1}{2}\mu_3 \pm \sqrt{\mu_3^2 - 4\omega_\theta^2} \quad (15.67)$$

have always negative real part. Hence, applying Theorems 4.16 and 4.18 in [7] it follows that for sufficiently small initial conditions of the error and internal dynamics  $\mathbf{e}(0)$ ,  $\boldsymbol{\eta}(0)$ , and for a small reference trajectory  $\omega_1(t)$  with small derivative, the state  $\boldsymbol{\eta}(t)$  will be bounded for all  $t \geq 0$ .  $\square$

*Remark 15.1.* Note that the proof about the local boundedness of the internal dynamics is valid only if the reference trajectory is small. If this is not the case the time-varying nonlinear system

$$\dot{\boldsymbol{\eta}} = \mathbf{f}_0(\boldsymbol{\eta}, \mathbf{y}_R(t)) \quad (15.68)$$

should be considered instead.

### 15.3.2 Parametric Resonance Stabilization

The choice of focusing on the frequency coupling condition allows to exploit the control law (15.57) also for stabilizing the system once parametric resonance has fully developed. This can be attained by defining a stabilizing trajectory  $\omega_S(t) \neq \frac{1}{2}\omega_e$  to be tracked by the closed-loop system. The control problem can be formulated as

**Parametric Resonance Stabilization.** Assume that  $\omega_e = 2\omega_\theta$  and that the system (15.16) is in parametric resonance. Given the stabilizing reference frequency  $\omega_S(t) = \bar{\omega} \neq \frac{1}{2}\omega_e(t)$ , find a control law  $\Phi_\delta^c = \Phi_\delta^c(\tilde{\mathbf{q}}, \dot{\tilde{\mathbf{q}}}, \omega_S(t))$  such that  $\omega_\theta$  converges asymptotically to  $\omega_S(t)$ .

The solution of the *Parametric Resonance Stabilization* problem results in designing the control law  $\Phi_\delta^c$  such that the length of the pendulum rod  $\delta$  converges to  $\delta^*$  for  $t \rightarrow \infty$ , where  $\delta^* = (\bar{l} - l_0)/l_0$  with  $\bar{l}$  being the length of the rod of a virtual pendulum oscillating at the natural frequency  $\bar{\omega}$ .

Note that since the stabilization is achieved by detuning the frequency coupling condition  $\omega_\theta = \frac{1}{2}\omega_e$  there is no need for controlling the horizontal position of the cart. Therefore in the following analysis it is assumed that the controller does not actuate the cart, which will remain at the position  $x = x^*$  where it was originally placed.

**Proposition 15.3.** *Assume that  $\omega_e = 2\omega_\theta$  and that the system in normal form (15.36)–(15.37) is in parametric resonance. Consider the reference vector  $\mathbf{y}_R = [y_{2R}(t), \dot{y}_{2R}(t)]^T = [x_4^*(t), x_8^*(t)]^T$ . The input–output feedback linearizing control law*

$$\mathbf{u} = \Gamma(\mathbf{x})^{-1}(\mathbf{v}(\mathbf{x}) + \mathbf{v}(\mathbf{x})\mathbf{w} + \phi(\mathbf{x})),$$

where

$$\phi(\mathbf{x}) = \mathbf{v} + \ddot{\mathbf{y}}_R(t)$$

solves the Parametric Resonance Stabilization problem and decouples the disturbance from the output  $y_2$ . Moreover the internal dynamics  $\dot{\eta} = \mathbf{f}_0(\eta, \xi)$  is bounded for all  $t \geq 0$ .

*Proof.* Analogously to the proof of Proposition 15.2 we define the tracking error as

$$\mathbf{e} = \begin{bmatrix} 0 \\ 0 \\ \xi_3 - y_{2R}(t) \\ \xi_4 - \dot{y}_{2R}(t) \end{bmatrix},$$

where the first two entries are equal to zero because the cart is assumed to maintain its position. The normal form (15.36) and (15.37) then reads

$$\dot{\eta} = \mathbf{f}_0(\eta, \mathbf{e} + \mathbf{y}_R), \quad (15.69)$$

$$\dot{\mathbf{e}} = \mathbf{A}_c \mathbf{e} + \mathbf{B}_c \Gamma(\mathbf{x}) \left\{ [\mathbf{u} - \mathbf{v}(\mathbf{x}) - \mathbf{v}(\mathbf{x})] - \begin{bmatrix} \ddot{y}_{1R} \\ \ddot{y}_{2R} \end{bmatrix} \right\}. \quad (15.70)$$

Therefore the state feedback control law

$$\mathbf{u} = \Gamma(\mathbf{x})^{-1}(\mathbf{v}(\mathbf{x}) + \mathbf{v}(\mathbf{x})\mathbf{w} + \phi(\mathbf{x})) \quad (15.71)$$

with  $\phi(\mathbf{x}) = -\mathbf{K}_S \mathbf{e} + [0, \dot{y}_{2R}]^T$  reduces the normal form to the cascade

$$\dot{\eta} = \mathbf{f}_0(\eta, \mathbf{e} + \mathbf{y}_R), \quad (15.72)$$

$$\dot{\mathbf{e}} = (\mathbf{A}_c - \mathbf{B}_c \mathbf{K}_S) \mathbf{e}, \quad (15.73)$$

where  $\mathbf{A}_c - \mathbf{B}_c \mathbf{K}_S$  is Hurwitz.

The boundedness of the internal dynamics  $\eta(t) = \mathbf{f}_0(\eta, \xi)$  can be demonstrated analogously as in Proposition 15.2.  $\square$

### 15.4 Simulation Results

The efficacy of the proposed control strategies for inducing and stabilizing parametric resonance has been tested in simulation.

Figure 15.3 shows an example of induction and tracking of parametric resonance. For  $0 < t < 100$  s the mass-spring-damper oscillates under the action of the external sinusoidal disturbance  $\Phi_y^e$  while the pendulum is at rest. At  $t = 100$  s a new reference trajectory  $\delta^*(t)$ , which ensures the tuning of the frequency coupling condition is provided. As a consequence, the controller (15.57) enforces that the output  $y_2(t)$  follows the reference trajectory and that the frequency condition for the onset of parametric resonance is fulfilled. At the same time the controller destabilizes the pendulum by driving the cart to its new set point  $x^*$ . This produces the sparkle for the onset of parametric resonance into the pendulum, which for  $100 \leq t < 400$  s develops oscillations of increasing amplitude at a frequency  $\omega_\theta = \frac{1}{2}\omega_{e,1}$ . At  $t = 400$  s the frequency of the external excitation decreases determining a temporary frequency ratio  $\omega_\theta/\omega_{e,2} = 1$  as shown in Fig. 15.4. Hence the controller increases the rod's length  $\delta$  up to the new reference trajectory maintaining the parametric resonance alive. The amplitude of the pendulum oscillations further increases due

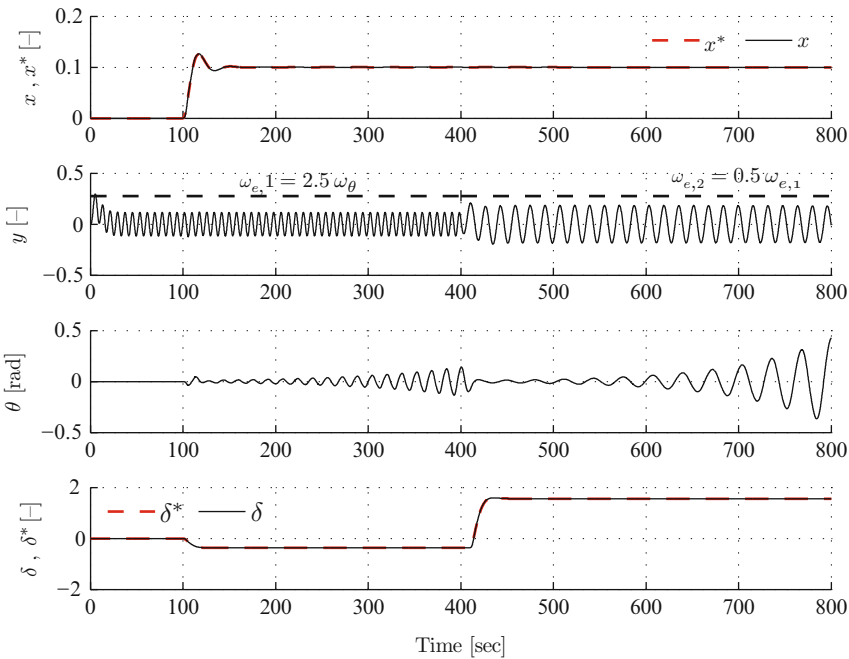


**Fig. 15.3** Parametric resonance tracking: multiple variations of external excitation frequency  $\omega_e$  are tracked by the controller

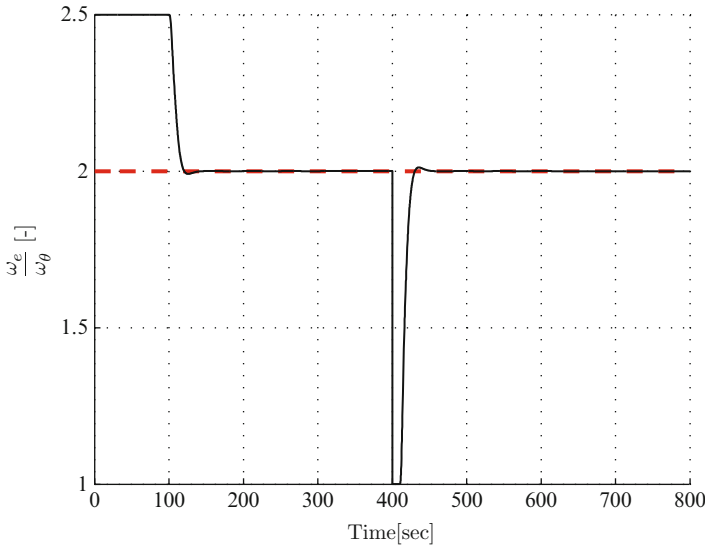


**Fig. 15.4** Parametric resonance tracking: the controller enforces that the frequency ratio  $\omega_e/\omega_\theta$  is kept equal to 2

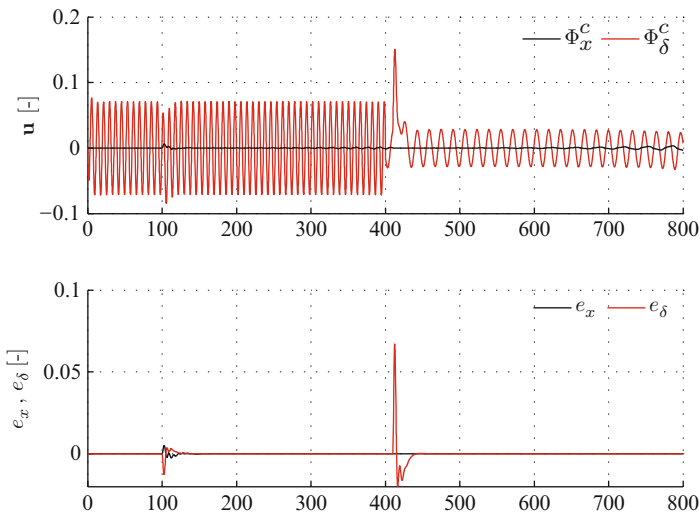


**Fig. 15.5** Parametric resonance tracking: (*top*) control signals and (*bottom*) position errors of the controlled variables

to the larger amplitude of the parametric excitation provided by  $y$ . Figure 15.5 illustrates the commanded control signals and the evolution of the position error.

Figure 15.6 shows an example of stabilization of parametric resonance after it has been triggered according to the former description. At  $t = 600s$  a stabilizing

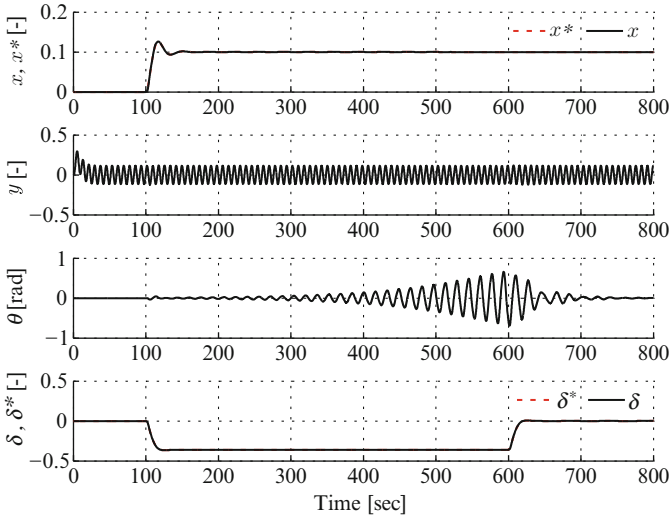


**Fig. 15.6** Parametric resonance stabilization: the controller stabilizes the pendulum about  $\theta = 0$  by detuning the frequency coupling condition

trajectory that detunes the frequency coupling condition is provided. Consequently, the controller (15.71) enforces the output  $y_2$  to track the new reference signal, and it brings the pendulum out of the principal parametric resonance condition within 200s. The decay rate of the pendulum oscillations could be increased if the proposed control strategy is coupled with a damping injection into the secondary system. This could be done by increasing the moment due to dissipative forces, for example, by applying a direct torque on the pendulum’s pivot point or by moving the cart in counter phase with respect to the pendulum oscillations.

## 15.5 Conclusions

Parametric resonance is a widespread phenomenon that may be threatening or beneficial according to the particular system where it takes place. A four degrees-of-freedom Lagrangian model of a pendulum with moving support has been derived in order to, first, revisit some of the stability theory of autoparametric resonant systems by applying Floquet theory, and, second, to design control strategies to induce and stabilize the unstable oscillations. Two control problems, namely the *Parametric Resonance Tracking* and the *Parametric Resonance Stabilization*, have been set up as output tracking problems where induction and stabilization of parametrically resonant behaviors are achieved by tracking a reference frequency, which enforces or not the frequency coupling condition  $\omega_\theta = \frac{1}{2}\omega_\lambda$ . An input–output feedback linearizing controller has been designed and analytically proven to

solve both control problems. The efficacy of the proposed control strategy has been also verified in simulation, where both induction and stabilization of parametric resonance into the pendulum with moving support have been successfully obtained.

The authors believe that control strategies aiming at inducing and tracking parametric resonance will be of particular interest for future application as energy conversion systems where the obvious goal is to increase the energy throughput while maintaining constant or even reducing the effort to produce such energy. In this respect parametric resonance can become a very useful phenomenon since very large oscillations can be generated by a rather small parametric excitation. However the same feature that makes parametric resonance appealing should create awareness of the potential danger hidden in such phenomenon. That is why a sound and profound knowledge of the dynamics of the system where parametric resonance is wished to be induced is needed in order to capture the energy flow between the different system modes when the resonance takes place. Therefore models and control methods which rely on the concept of energy exchange in the system and through interacting systems seems to be particularly suited for these kinds of applications.

## References

1. Boyd, J.P.: Chebyshev and Fourier Spectral Methods. DOVER Publications (2000)
2. Breu, D., Fossen, T.I.: Extremum seeking speed and heading control applied to parametric roll resonance. In: Proceedings of the 8th IFAC Conference on Control Applications in Marine Systems. IFAC, Germany (2010)
3. Galeazzi, R., Holden, C., Blanke, M., Fossen, T.I.: Stabilization of parametric roll resonance by combined speed and fin stabilizer control. In: Proceedings of the 10th European Control Conference. EUCA, Hungary (2009)
4. Grimshaw, R.: Nonlinear Ordinary Differential Equations. CRC Press, United States of America (1993)
5. Holden, C., Galeazzi, R., Perez, T., Fossen, T.I.: Stabilization of parametric roll resonance with active U-tanks via Lyapunov control design. In: Proceedings of the 10th European Control Conference. EUCA, Hungary (2009)
6. Isidori, A.: Nonlinear Control Systems – Third Edition. Springer, Great Britain (1995)
7. Khalil, H.K.: Nonlinear Systems – third edition. Prentice Hall, United States of America (2002)
8. Limebeer, D.J.N., Sharp, R.S., Evangelou, S.: Motorcycle steering oscillations due to road profiling. Transactions of the ASME **69**, 724–739 (2002)
9. Mathieu, E.: Mémoire sur le mouvement vibratoire d'une membrane de forme elliptique. Journal de Mathématiques Pures et Appliquées **13**, 137–203 (1868)
10. Olvera, A., Prado, E., Czitrom, S.: Performance improvement of OWC systems by parametric resonance. In: Proceedings of the 4th European Wave Energy Conference (2001)
11. Olvera, A., Prado, E., Czitrom, S.: Parametric resonance in an oscillating water column. Journal of Engineering Mathematics **57**(1), 1–21 (2007)
12. Oropeza-Ramos, L.A., Burgner, C.B., Turner, K.L.: Robust micro-rate sensor actuated by parametric resonance. Sensors and Actuators A: Physical **152**, 80–87 (2009)
13. Shaeri, A., Limebeer, D.J.N., Sharp, R.S.: Nonlinear steering oscillations of motorcycles. In: Proceedings of the 43rd IEEE Conference on Decision and Control. IEEE, United States of America (2004)

14. Tondl, A., Ruijgrok, T., Verhulst, F., Nabergoj, R.: *Autoparametric Resonance in Mechanical Systems*. Cambridge University Press, United States of America (2000)
15. Trefethen, L.N.: *Spectral methods in MATLAB*. SIAM (2000)
16. Turner, K.L., Miller, S.A., Hartwell, P.G., MacDonald, N.C., Strogatz, S.H., Adams, S.G.: Five parametric resonances in a microelectromechanical system. *Nature* **396**, 149–152 (1998)
17. Zhang, W., Turner, K.L.: Application of parametric resonance amplification in a single-crystal silicon micro-oscillator based mass sensor. *Sensors and Actuators A: Physical* **122**, 23–30 (2005)